UNCLASSIFIED
SECURITY CLASSIFICATION OF THIS PAGE

REPORT DOCUMENTATION PAGE

Form Approved OMB No. 0704-0188

1a. REPORT SECURITY CLASSIFICATION: Unclassified	1b. RESTRICTIVE MARKINGS
AD-A220 185	3. DISTRIBUTION / AVAILABILITY OF REPORT: Approved for public release; distribution unlimited.
4. PERFORMING ORGANIZATION REPORT NUMBER(S)	5. MONITORING ORGANIZATION REPORT NUMBER(S)
6a. NAME OF PERFORMING ORGANIZATION: Research Laboratory of Electronics, Massachusetts Institute of Technology	6b. OFFICE SYMBOL (If applicable)
7a. NAME OF MONITORING ORGANIZATION	
6c. ADDRESS (City, State, and ZIP Code): 77 Massachusetts Avenue, Cambridge, MA 02139	7b. ADDRESS (City, State, and ZIP Code)
8a. NAME OF FUNDING / SPONSORING ORGANIZATION: Office of Naval Research	8b. OFFICE SYMBOL (If applicable)
9. PROCUREMENT INSTRUMENT IDENTIFICATION NUMBER: N00014-89-J-1654	
8c. ADDRESS (City, State, and ZIP Code): 800 North Quincy St., Arlington, VA 22217	10. SOURCE OF FUNDING NUMBERS

PROGRAM ELEMENT NO.	PROJECT NO.	TASK NO.	WORK UNIT ACCESSION NO.
	4127794--	02	

11. TITLE (Include Security Classification): Microwigglers for Submillimeter Wavelength Free-Electron Lasers

12. PERSONAL AUTHOR(S): Prof. George Bekefi

13a. TYPE OF REPORT	13b. TIME COVERED	14. DATE OF REPORT (Year, Month, Day)	15. PAGE COUNT
Annual	FROM 2-1-89 TO 1-31-90	March 28, 1990	

16. SUPPLEMENTARY NOTATION

17. COSATI CODES			18. SUBJECT TERMS (Continue on reverse if necessary and identify by block number)
FIELD	GROUP	SUB-GROUP	

19. ABSTRACT (Continue on reverse if necessary and identify by block number)

The work of George Bekefi and his collaborators is summarized here.

20. DISTRIBUTION / AVAILABILITY OF ABSTRACT	21. ABSTRACT SECURITY CLASSIFICATION
☒ UNCLASSIFIED/UNLIMITED ☐ SAME AS RPT. ☐ DTIC USERS	Unclassified

22a. NAME OF RESPONSIBLE INDIVIDUAL	22b. TELEPHONE (Include Area Code)	22c. OFFICE SYMBOL
Mary Greene - RLE Contract Reports	(617) 258-5871	

DD Form 1473, JUN 86 — Previous editions are obsolete. — SECURITY CLASSIFICATION OF THIS PAGE: UNCLASSIFIED

Annual Scientific Report on Grant No. N00014-89-J-1654

for research on

Microwigglers for Submillimeter Wavelength Free-Electron Lasers

for the period

1 February 1989 - 31 January 1990

Submitted by George Bekefi

March 28, 1990

Massachusetts Institute of Technology
Research Laboratory of Electronics
Cambridge, Mass. 02139

During the past year we have made significant progress in the design of a 75-period microwiggler and have tested the prototype. A detailed report of this work is attached.

We expect that the construction of the actual wiggler and the power supply will be finished by early fall of 1990. At that time the microwiggler will be incorporated into the Brookhaven National Laboratory's 50 MeV rf linac program. Spontaneous and stimulated radiation measurements will begin when it is installed.

A Planar Electromagnet Microwiggler for Free Electron Lasers*

R. Stoner, S.C. Chen and G. Bekefi

Department of Physics,
Research Laboratory of Electronics
and
Plasma Fusion Center
Massachusetts Institute of Technology
Cambridge, Massachusetts 02139

Abstract

We have designed and tested an electromagnet planar microwiggler for use in free-electron lasers (FELs), constructed of current conductors wound on ferromagnetic cores. A prototype with a period of 1 cm and gap of 0.5 cm produced a peak field on axis in excess of 4.6 kG, with a linear B/H characteristic to about 3.2 kG. The field of each half-period of the wiggler is independently tuneable by adjusting the current delivered to each, thus allowing for precision tuning and/or wiggler tapering. We employ general scaling laws to predict performance of a geometrically similar design with a period of 5 mm.

*This work was supported by the Office of Naval Research.

1. Introduction

Short-period (1-10 mm) wigglers for free electron laser (FEL) applications have been a subject of considerable interest [1-6]. The use of such a microwiggler permits higher-frequency radiation to be generated with a device that is more compact than one employing wigglers of standard lengths (typically 3-10 cm).

Reduced length scales imply that fabrication imperfections become increasingly more serious. Field amplitude tuneability, as a means of compensating for the resulting random field errors, becomes a particularly important attribute for a microwiggler design. Field amplitude tuneability also has general usefulness for applications like field tapering for FEL efficiency enhancement. The use of electromagnets permits such tuneability; moreover, a planar geometry wiggler readily lends itself to a tuneable configuration, inasmuch as it can be made of discrete electromagnets.

This paper describes a new planar electromagnet microwiggler design and the measurements of its performance. The work is an outgrowth of earlier studies [6]. Sec. 2 presents experimental results; Sec. 3 discusses the design of our new prototype test piece, and uses general scaling laws to predict performance of geometrically similar designs at reduced length scales. It is shown that the attainable time-averaged value of the magnetic field in pulsed-mode operation remains constant as size is decreased.

2. Experimental Results

We have constructed a four-period microwiggler prototype with period 10.2 mm, gap 5.1 mm, consisting of 16 wire-coil electromagnets wound on laminated Microsil (silicon-iron) cores (Magnetic Metals, Inc). Each core consists of seven laminations of dimension 1.27 cm x 3.18cm x .0356 cm. Fig. 1 illustrates the geometry. The test piece has tuneable amplitude, with current delivered to each half-period adjustable by means of a precision potentiometer. Each coil consists of 50 turns of 32 AWG copper wire (.0202 cm dia.) and has a resistance of 2.0 ohms. The coils are connected in parallel and the wiggler is energized by a simple pulser circuit consisting of an air-core inductor (L = 1.3 mH) and a bank of six 1500-microfarad capacitors connected in parallel. The resulting waveform is an underdamped sine wave. The pulser is fired by an SCR, which

commutates off at the first zero- crossing of the current. Hence, the wiggler is energized by a single positive current pulse. The full period of the underdamped waveform is about 22 msec.

Wiggler field amplitude as a function of input current density was measured and is shown plotted in Fig. 2. The results of a POISSON simulation are seen to match the data quite well– this is partly fortuitous since we made no effort to model the permeability of our particular material. The probe was located at a peak near the central part of the wiggler; the input current was measured using a Rogowski coil and the field was measured by means of a Hall probe gaussmeter, using a specially designed miniature probing tip. The current values shown are those borne by the 32 AWG wire: a current of 20 amps corresponds to a current density of 3.12×10^4 amps/cm^2.

Note that B as a function of I is quite linear to about 3.2 kG. The 3 kG linear field regime of our design extends further than those of ferro-core designs reported previously [1,2,6]. Fig. 3 shows a POISSON-generated flux map of our prototype in its linear B/I regime. The regions of highest flux density in the cores occur inside the windings, which are thus purposely displaced toward the polefaces relative to the center of the cores. The closer to the polefaces the highest flux density region occurs, the higher will be the fields at the polefaces (and on the wiggler axis) when the core saturates. The windings do not extend along the entire ferro-core, since in such a configuration the highest flux density occurs at the center of the cores, well back from the polefaces, leading to onset of saturation at relatively low field levels.

Fig. 4 shows the prototype's measured untuned on-axis magnetic field profile. POISSON calculations of the peak fields are also shown. There is very little higher harmonic content in the field. This is mainly due to the large gap-to-period ratio: the field at a given point on the wiggler axis is the sum of contributions from many half-period elements. The wiggler end effects are quite modest, due to the favorable symmetry of the current density about the central plane perpendicular to the wiggler (z) axis, as will be mentioned in Sec. III. In the absence of tuning, we observe random field amplitude errors in the prototype of $\pm 4\%$; this is a reasonable value considering the very simple methods used in its construction.

Random field errors as well as undesired systematic finite wiggler effects are sharply

reduced by tuning. The results of profile tuning experiments are shown in Fig. 5. Fig. 5(a) is a plot of the prototype's on-axis magnetic field, tuned to a constant-amplitude profile. Random field errors are 0.4 % RMS, with a maximum deviation from constant amplitude of 0.6 %. Amplitude tuning has therefore reduced random field errors by an order of magnitude. Minor improvements in the tuning regimen should permit further reduction of random errors, perhaps to the level of 0.2 % RMS. Fig. 5(b) is a measured profile demonstrating the capability of adiabatic field up-taper for improved e-beam coupling into the wiggler. The magnet was DC-energized with about 0.5 amperes per coil (for a total of 8.0 amperes) during the tuning and profile measurements.

Fig. 6 is a plot of the measured wiggler field profile across the gap along a line from poleface center to poleface center. The data are again fortuitously well matched by the POISSON code (using its standard permeability table) and are also well represented by a hyperbolic cosine curve, in agreement with expectations. The distance over which measurements could be taken was restricted by the Hall probe hitting the polefaces.

Heat generation, even under pulsed conditions of the wiggler, is, of course, of major concern. A simple calculation shows that the I^2 R heating induced by the underdamped waveform with maximum current I_{max} is equivalent to that induced by a square pulse of height I_{max} and duration 5 msec. Even with this long pulse, the maximum peak field value shown in Fig. 4, 4.6 kG, is not the highest attainable field. At I = 57 amps, (I^2R·5 msec) corresponds to a temperature increase of 80° C (we have found the Formvar insulation to be reliable to around 100° C– 80° above typical ambient temperature of 20° C), so that (from a rough extrapolation of the measurements of Fig. 4) 5 msec field pulses of 5 kG are clearly attainable. For a wiggler of 50 periods, a 11.4 kA pulser is required in order to provide 57 amperes per coil, and given the modest voltages involved (less than 0.5 kV), its construction poses no special difficulties. It is then reasonable to claim 5.0 kG as a practical maximum attainable field from a full 50-period wiggler in long-pulse operation. For short-pulse operation, higher fields could be attained, but current and voltage requirements become formidable as the ferro-cores saturate.

For extremely short pulse duration, and very high fields, a pulsed-wire geometry with no ferro-cores may well be preferable [7]. Nevertheless, the ferro-core design

can produce a 3 kG square pulse of 40 msec duration, while a reasonable pulsed-wire design could produce such a pulse for only a fifth of that time. Using more exotic, high-μ materials could likely make attainable 3 kG pulses of 0.1 sec duration in a magnet with gap-to-period ratio of 0.5.

3. Design Discussion

To aid us in our design, we began by leaving out the ferromagnetic cores. Fig. 7 illustrates an infinite 2-D array of parallel rectangular conductors, carrying currents of identical magnitude in a configuration that produces a periodic magnetic field on the axis of the structure. Expressing the current density in terms of a Fourier transform permits the calculation of an exact analytical expression for the magnetic field: an expression for the field valid inside the wiggler gap (i.e., between the two planes of conductors) is

$$B_y = \frac{8j\lambda}{\pi c} \sum_{\substack{n>0 \\ n \text{ odd}}} \frac{1}{n^2} \sin\frac{n\pi}{2} \sin\frac{n\pi W}{\lambda}(1 - e^{-2\pi T/\lambda})e^{-\pi G/\lambda} \cos\frac{2\pi z}{\lambda} \cosh\frac{2\pi y}{\lambda}$$

$$B_z = -\frac{8j\lambda}{\pi c} \sum_{\substack{n>0 \\ n \text{ odd}}} \frac{1}{n^2} \sin\frac{n\pi}{2} \sin\frac{n\pi W}{\lambda}(1 - e^{-2\pi T/\lambda})e^{-\pi G/\lambda} \sin\frac{2\pi z}{\lambda} \sinh\frac{2\pi y}{\lambda} \qquad (1)$$

Here c is the speed of light and j the current density in the windings. G is the gap spacing and λ the wiggler periodicity. T is the winding thickness in the y direction and W is the winding thickness in the z direction with $(\lambda - W)/2$ as the core thickness to be inserted (see Fig. 7). This result illustrates well-known general properties of planar wigglers: exponential decrease in field magnitudes with increasing (G/λ), and the absence of even harmonics in the field. It is also interesting to note that Eq. (1) has precisely the same form as the expression for the magnetic field due to rare-earth cobalt (REC) magnets in the Halbach configuration [8], to an overall multiplicative constant (REC magnetization being analogous to electromagnet current), except that the REC magnetic field harmonics fall off as $1/n$ instead of $1/n^2$. Simulations reveal that a finite structure with a current distribution symmetric in z and having half-width

conductors at the ends produces a field closely modeled by Eq. (1) at points more than a couple of periods in from the ends of the structure.

Eq. (1) predicts that a pulsed-wire design with $\lambda = 1.0$ cm, $G = 0.5$ cm, $W = 0.211$ cm, and $T = 0.211$ cm (81 turns of 32 AWG wire per coil) will produce 68 G of magnetic field on axis per ampere of current. Addition of ferromagnetic cores substantially increases B/I efficiency, and in fact we produced 150 G/ampere as described in Sec. 2. Improved field per unit input current density is not the only reason for including ferro-cores: the ferro-cores can be embedded in an external matrix formed with very high precision, thus precisely fixing the core positions. Inasmuch as fully two-thirds of the magnetic field in the linear B/H regime in our design is due to induced magnetization currents in the ferro-cores, there is great advantage in field precision to be gained by locating them precisely. Moreover, cumulative field periodicity errors occurring in ferro-core/solid-conductor stack designs [2] are eliminated by embedding the cores in an external matrix, which can only be done if the ferro-cores extend beyond the conductors as in our design. Thus we see an additional advantage of placing the conductors at the polefaces and extending the cores beyond the conductors, in addition to the saturation advantage described in Sec. 2.

The relative "width" along the z-axis of the ferro-cores and wires was determined empirically by numerical simulations: the width with the best saturation characteristic was found, and then T was reduced to the point where the B/I efficiency in the linear regime was about 150 G/(amp into 32 AWG coil wire). It was observed that increasing T for fixed wire diameter and ferro-core widths increased B/I efficiency but lowered the field value at which saturation occurred. The B/I efficiency grew roughly linearly with T, and the product of the efficiency and the saturation field was roughly constant.

We are also considering the construction of a 5 mm-period wiggler, using the geometry of our 10 mm-period prototype with all length factors reduced by a factor of 2. Simple scaling laws can be used to predict the performance of geometrically similar designs (i.e., all lengths scaled by the same factor). Eq. (1) shows the peak field magnitude scales as

$$| \vec{B} | = j\lambda f(G/\lambda, T/\lambda, W/\lambda) \qquad (2)$$

for the simple pulsed-wire design; it can easily be shown that a ferro-core system in its linear B/H regime has the same kind of scaling [9]. That is, the field magnitude scales like ($j \cdot \lambda$·function invariant under length scale). The 5 mm-period design then requires twice the current density to attain a given field level, compared to the 10 mm-period design. Therefore, to maintain a given field amplitude and a given conductor temperature increase per shot, field pulse durations must be reduced by a factor of 4 in the 5 mm-period design.

The saturation field of the 5 mm-period design is the same as that of the 10 mm-period design, and the (L/R) rise time of the 5 mm-period structure (in the linear B/H regime) is 1/4 that of the 10 mm-period system. One can also prove that the characteristic conduction cooling time of the 5 mm-period structure is 1/4 that of the 10 mm-period design.

The factor-of-four reduction in the cooling time permits the 5-mm period device to operate at four times the the pulse repetition frequency of the 10 mm-period design, assuming a fixed temperature increase per pulse. This more rapid pulsing rate is possible because the (L/R) rise time is four times smaller in the smaller structure and so the time scale of the current waveform can be compressed. Reducing the length of each pulse by a factor of four permits doubling of the current density with no change in the temperature increase per pulse, so that the same $\mid \vec{B} \mid$ can be attained during the shorter pulse in the smaller structure. This implies that the smaller structure can produce magnetic field pulses of a given magnitude having 1/4 the pulse length at four times the rate–so that the time-averaged $\mid \vec{B} \mid$ attainable by the 10 mm-period design can also be generated by a 5 mm-period wiggler.

The wiggler parameter K (also called a_w), defined by [10]

$$K = \frac{eB_w\lambda_w}{2\pi mc^2}, \tag{3}$$

figures prominently in efficiency enhancement schemes using wiggler tapering to maintain resonance as the electrons' energy is radiated and γ decreases [10]:

$$\lambda_{res} = \frac{\lambda_w(1 + (K^2/2))}{2\gamma^2} \tag{4}$$

Our design permits high-precision wiggler amplitude down-tapering. It must be noted, however, that for periods much shorter than 1 cm, K becomes too small (e.g., $K = 0.23$ at $\lambda_w = 5$ mm) so that amplitude tapering is of dubious usefulness since the "dynamic range" of K^2 is now very limited.

An important limitation of ferro-core electromagnet wigglers is that they are largely incompatible with externally applied magnetic fields, e.g., a quadrupole field for beam focussing. This limitation can be circumvented in part by employing two-plane wiggler focussing schemes in which the planar geometry is modified, such as poleface shaping or poleface canting [11], to obviate the need for external focussing.

4. Conclusion

We have built a 4-period microwiggler prototype with a 10.2 mm period and a 5.1 mm gap, using a design which permitted attainment of 3.2 kG on-axis peak magnetic fields in the linear B/H regime, while preserving good B/I efficiency for generation of long (40 msec at 3 kG) magnetic field pulses. In this regime fine tuning of the wiggler is readily achieved by varying the current in the individual elements. Fields exceeding 4.6 kG in the saturated B/H regime were observed. When precise tuning of the wiggler is not an issue, operation in the saturated regime may well yield magnetic fields as high as 5 kG. A measured profile of the field taken along the wiggler axis shows good agreement with numerical simulations. End effects are minimal. Tuning is shown to dramatically improve field uniformity, reducing random field errors by an order of magnitude, from $\pm 4\%$ in the untuned profile to $\pm 0.4\%$ in the tuned case. A measured profile of the field taken across the wiggler gap also shows good agreement with computational predictions.

We have developed a simple design regimen for pulsed-wire planar wigglers based on analytic expressions for magnetic fields and L/R rise times which we used as a conceptual basis for our ferromagnetic core-based design. We have briefly discussed our design procedure, and used general scaling laws to predict the performance of a geometrically similar design with 5 mm period and 2.5 mm gap. We show that the smaller structure should be able to produce the same time-averaged magnetic field as

the 10 mm period design in pulsed-mode operation.

References

1. S.C. Chen, G. Bekefi, S. DiCecca and A.C. Wang, Proceedings of the Tenth International Conference on FEL, Jerusalem, Israel, 1988 (North Holland, to be published).

2. J.H. Booske, W.W. Destler, Z. Segalov, D.J. Racack, E.T. Rosenbury, T.M. Antonsen, Jr., V.L. Granatstein and I.D. Mayergoyz, J. Appl. Phys. **64**, 6 (1988) and the references therein.

3. R.M. White, Appl. Phys. Lett. **46**, 194 (1985).

4. G. Ramian, L. Elias and I.Kimel, Nucl. Instr. Methods Phys. Res. **A250**, 125 (1986).

5. B.G. Danly, G. Bekefi, R.C. Davidson, R.J. Temkin, T.M. Tran and J.S. Wurtele, IEEE J. Quant. Electron. **QE-23**, 103 (1987).

6. S.C. Chen, G. Bekefi, S. DiCecca and R. Temkin, Appl. Phys. Lett. **46**, 1299 (1989).

7. R. W. Warren (private communication).

8. K. Halbach, Nucl. Instr. Methods Phys. Res. **187**, 109 (1981)

9. J.Slater, 11th International Conference on Free Electron Lasers (1989)

10. T.C. Marshall, *Free Electron Lasers*, Macmillan (1985) pp. 20-23

11. K.E.Robinson and D.C.Quimby, Proc. IEEE Particle Accel. Conf., 428 (1987)

Figure Captions

Figure 1. Geometry of the microwiggler test piece. The coordinate axes as well as definitions of design parameters are shown. The arrows inscribed on the copper windings indicate direction of current flow.

Figure 2. Wiggler field amplitude as a function of current density. Measured data and POISSON calculations are shown.

Figure 3. POISSON-generated equipotential map for the MIT prototype. The field map shown corresponds to the linear B/H regime.

Figure 4. Measured wiggler field profile taken along the wiggler (z) axis, without tuning. The continuous curve is the measured data; POISSON-calculated values for the peaks are shown as crosses.

Figure 5. Measured wiggler field profiles taken along the wiggler (z) axis, with tuning. A constant amplitude profile is shown in (a). The amplitude is constant to 0.4% RMS with a maximum deviation of 0.6%. A "linear ramp" profile is shown in (b), which demonstrates the capability for adiabatic up-taper for wiggler/e-beam matching.

Figure 6. Measured wiggler field profile taken across the wiggler gap from poleface center to poleface center. Data is normalized to the value of the field at gap center. A POISSON calculation of the field profile is shown, as well as the hyperbolic cosine function that best fits the data.

Figure 7. 2-D planar wiggler structure without ferro-cores. Coordinate axes and parameter definitions are shown. The structure is taken to be infinite in extent along the x-direction (perpendicular to the page), and infinite and periodic along the z-direction (wiggler axis). The conductors carry uniform currents of identical magnitude in the directions indicated.

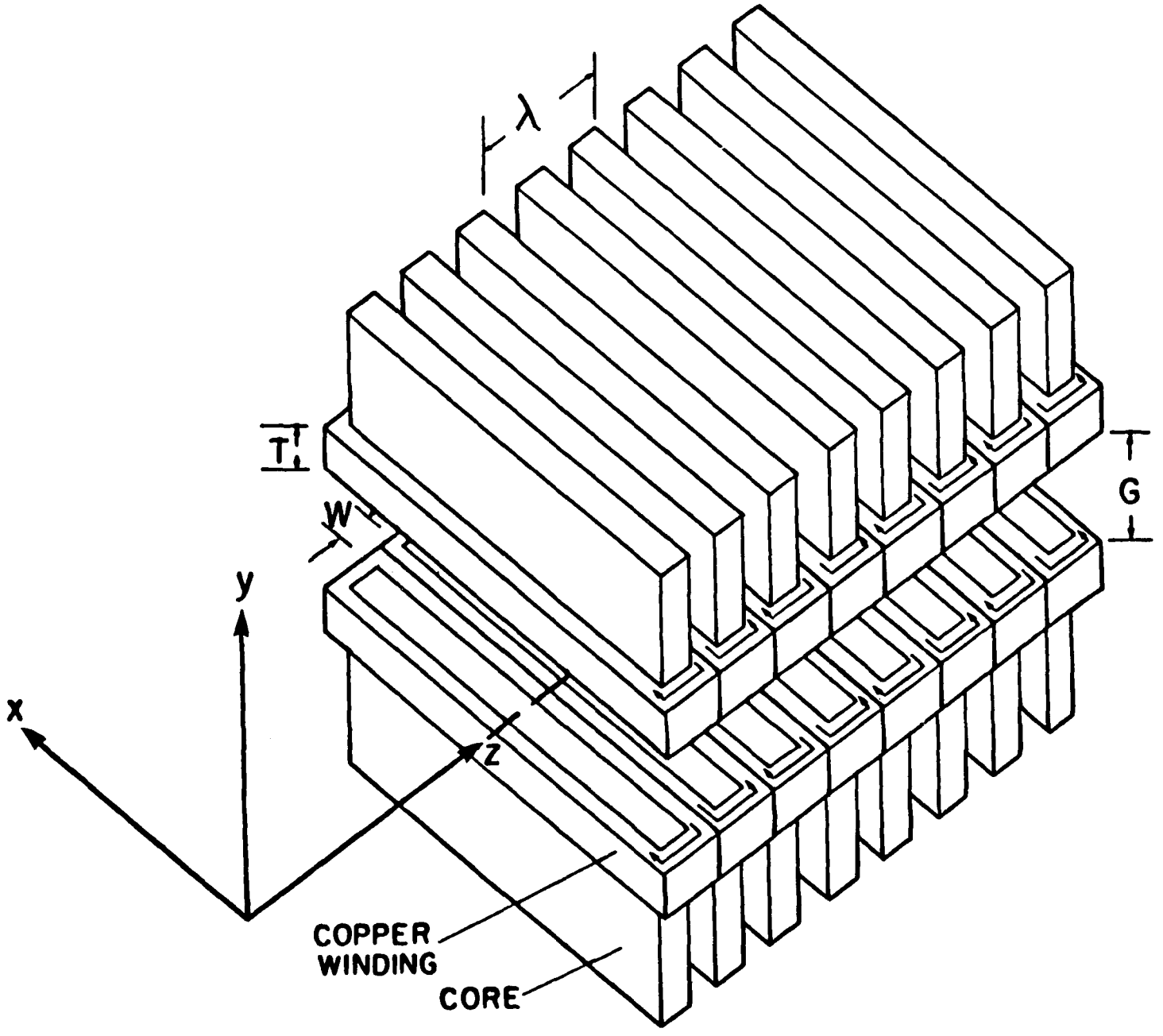

Figure 1

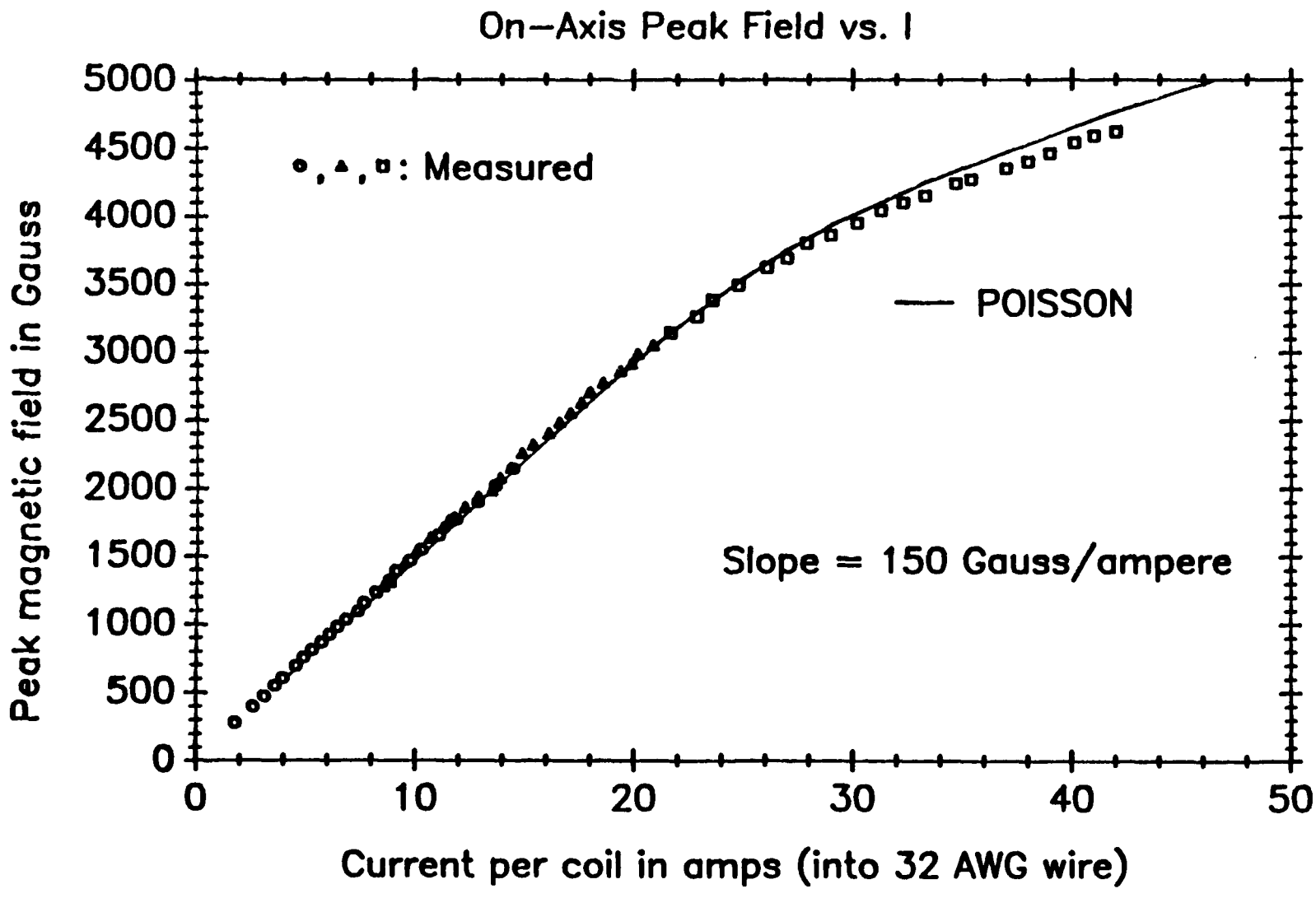
On–Axis Peak Field vs. I
Peak magnetic field in Gauss
5000
4500
4000
3500
3000
2500
2000
1500
1000
500
0
0
10
20
30
40
50
Current per coil in amps (into 32 AWG wire)
o, ▲, ▫: Measured
— POISSON
Slope = 150 Gauss/ampere

Figure 2

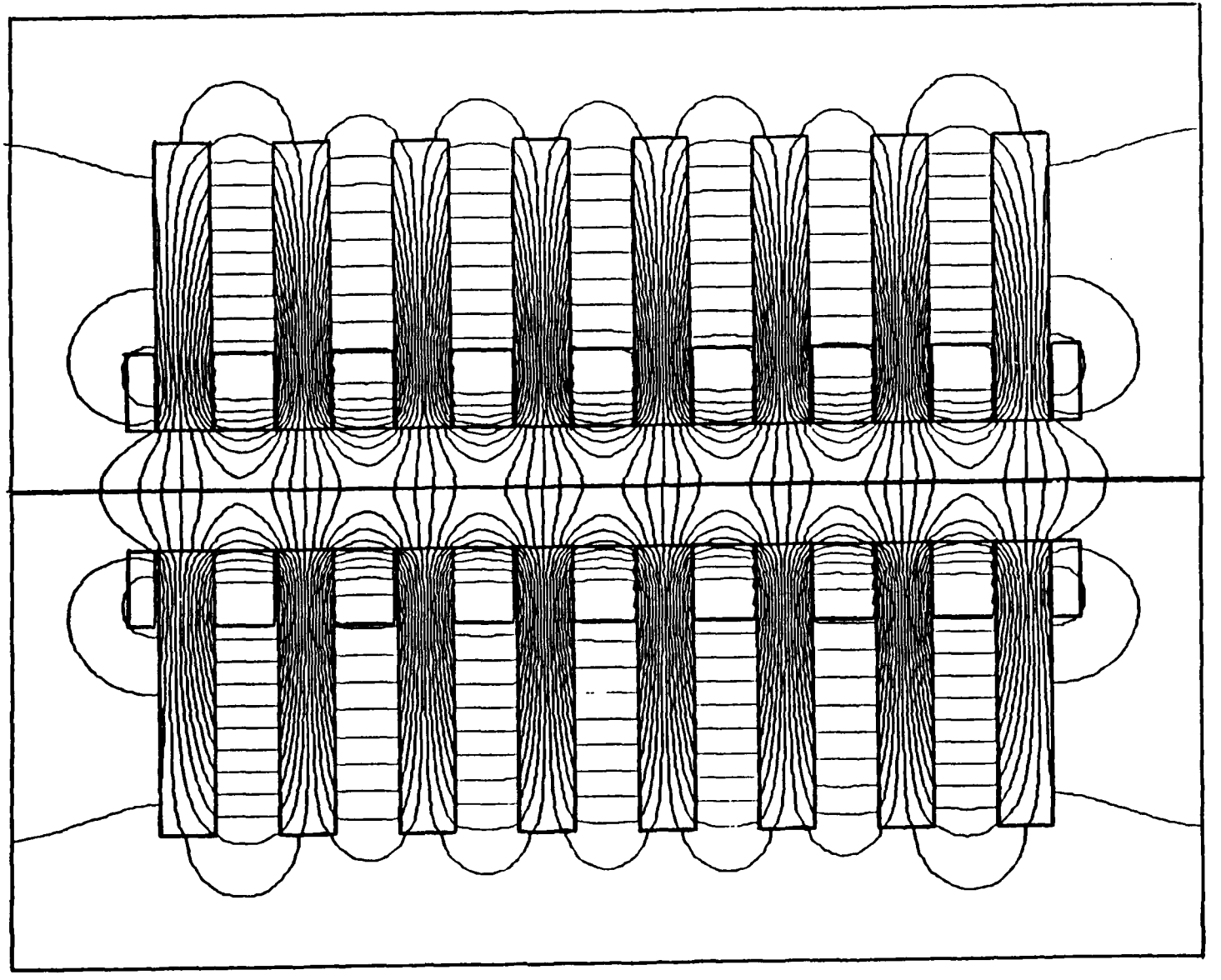

Figure 3

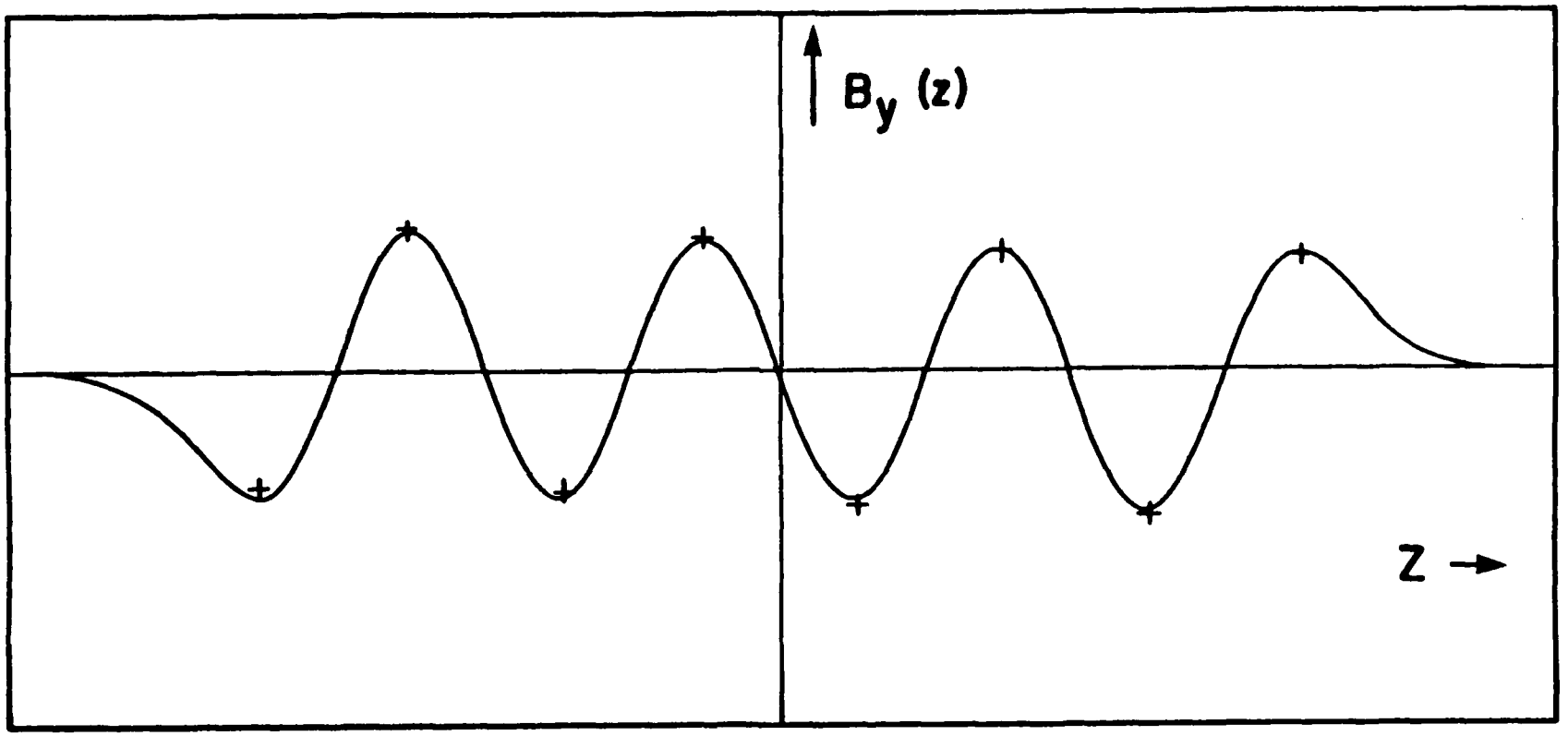

Figure 4

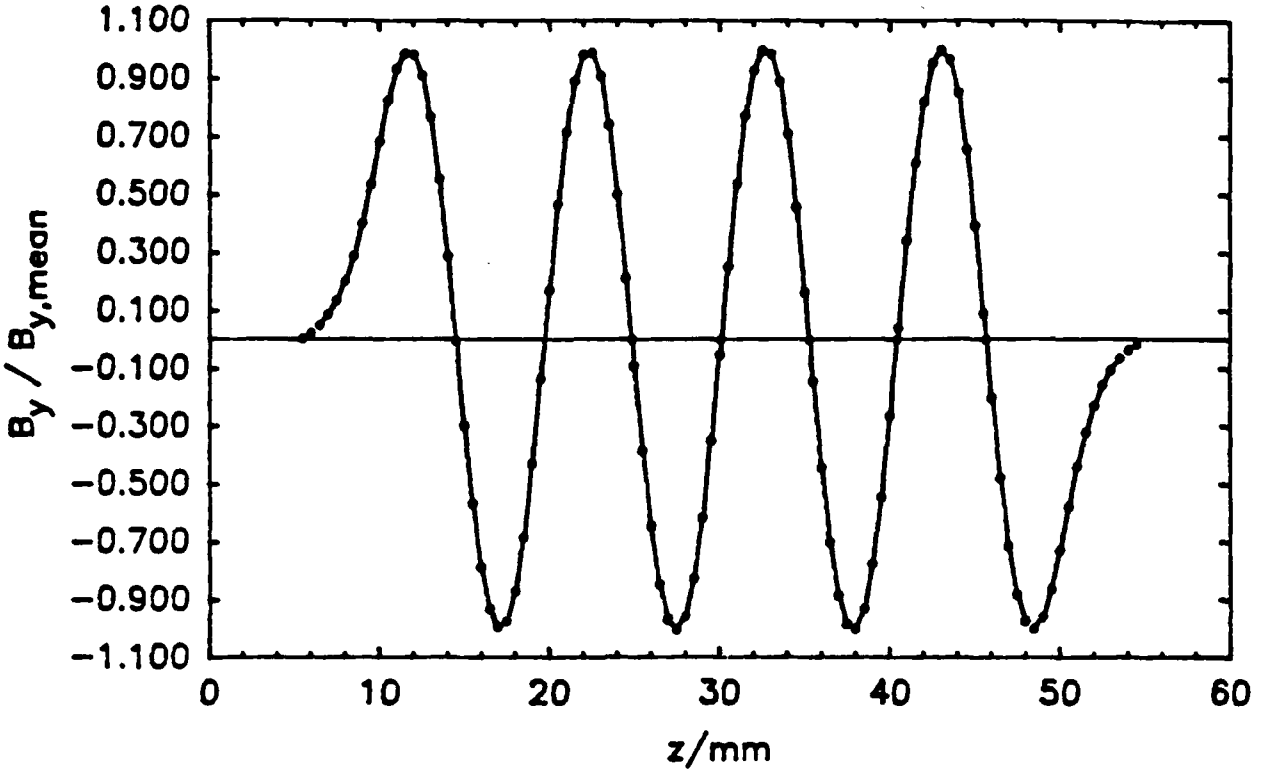

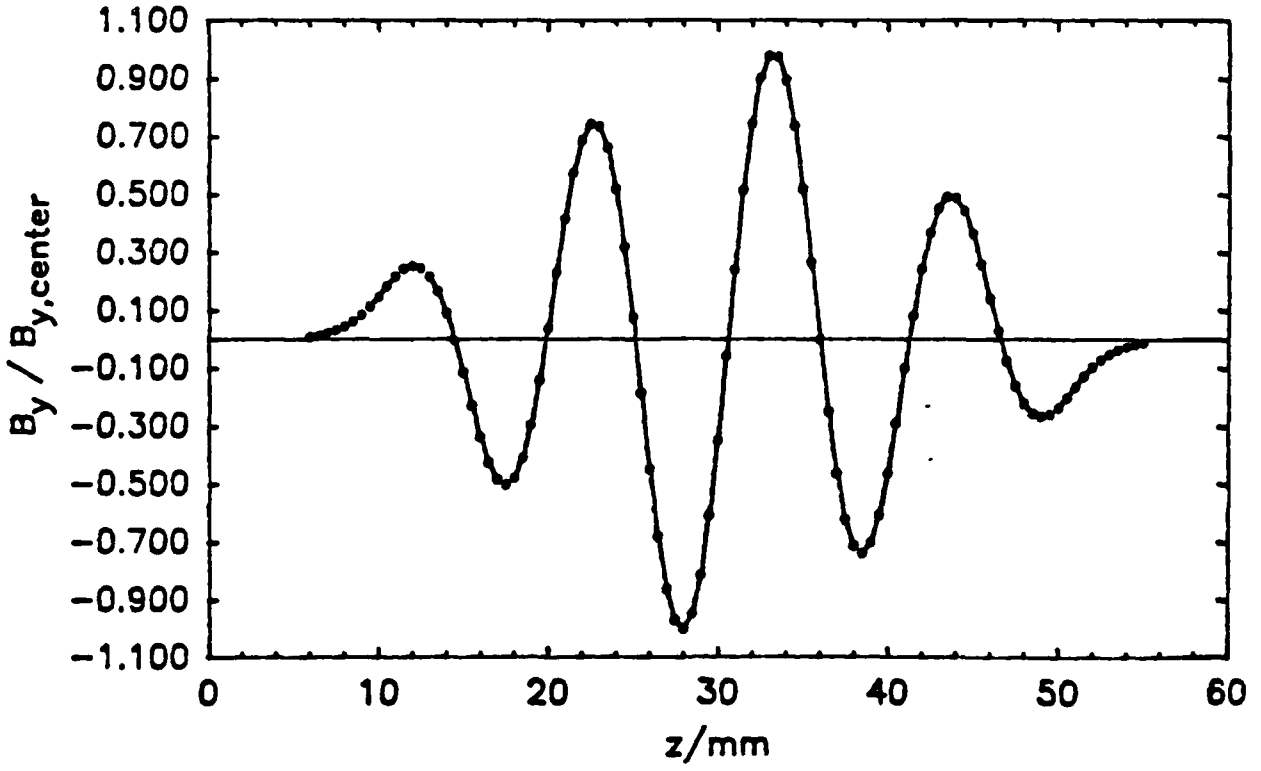

Figure 5a (above)
Figure 5b (below)

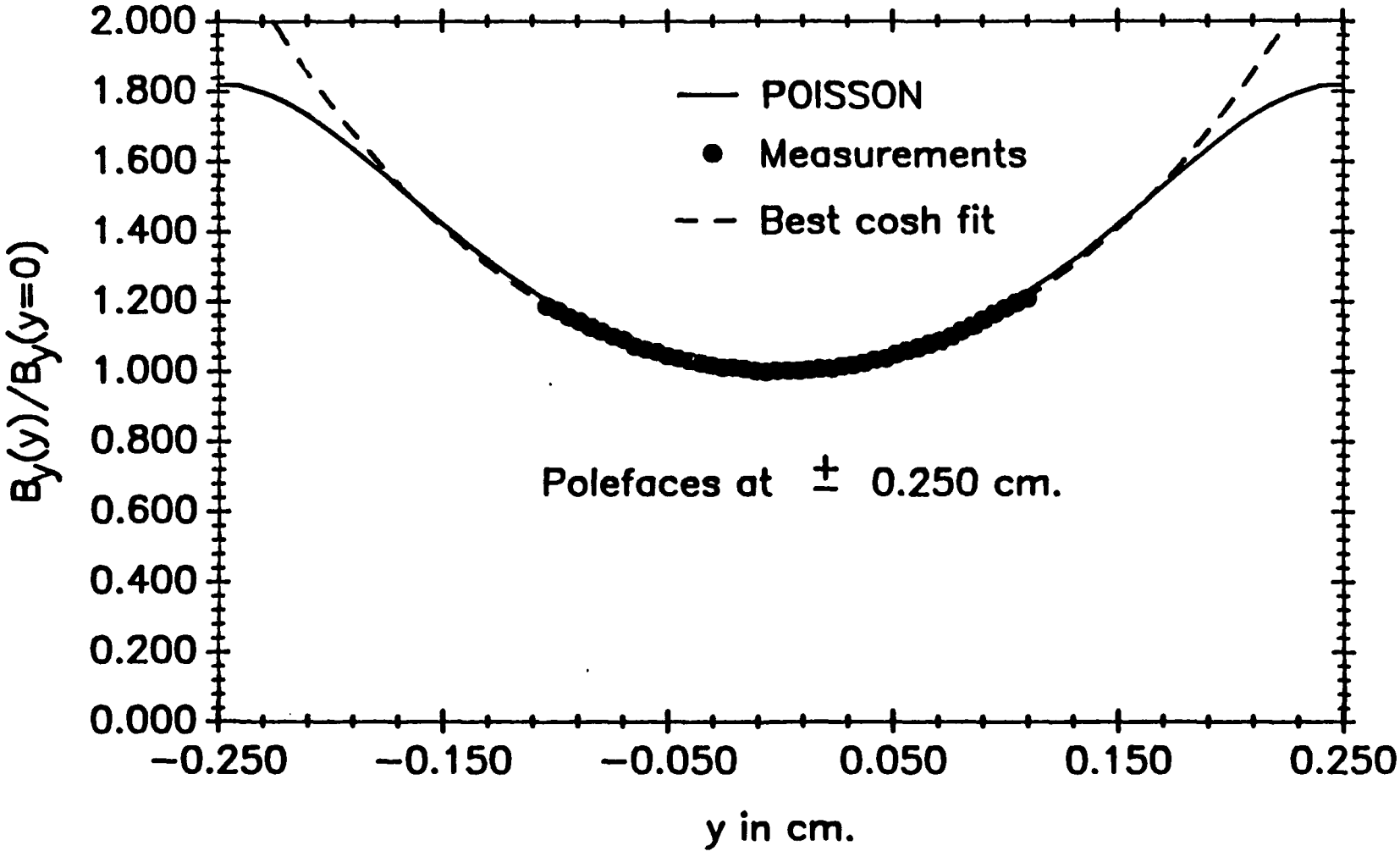
2.000
1.800
1.600
1.400
1.200
1.000
0.800
0.600
0.400
0.200
0.000
$B_y(y)/B_y(y=0)$
POISSON
Measurements
Best cosh fit
Polefaces at ± 0.250 cm.
−0.250
−0.150
−0.050
0.050
0.150
0.250
y in cm.

Figure 6

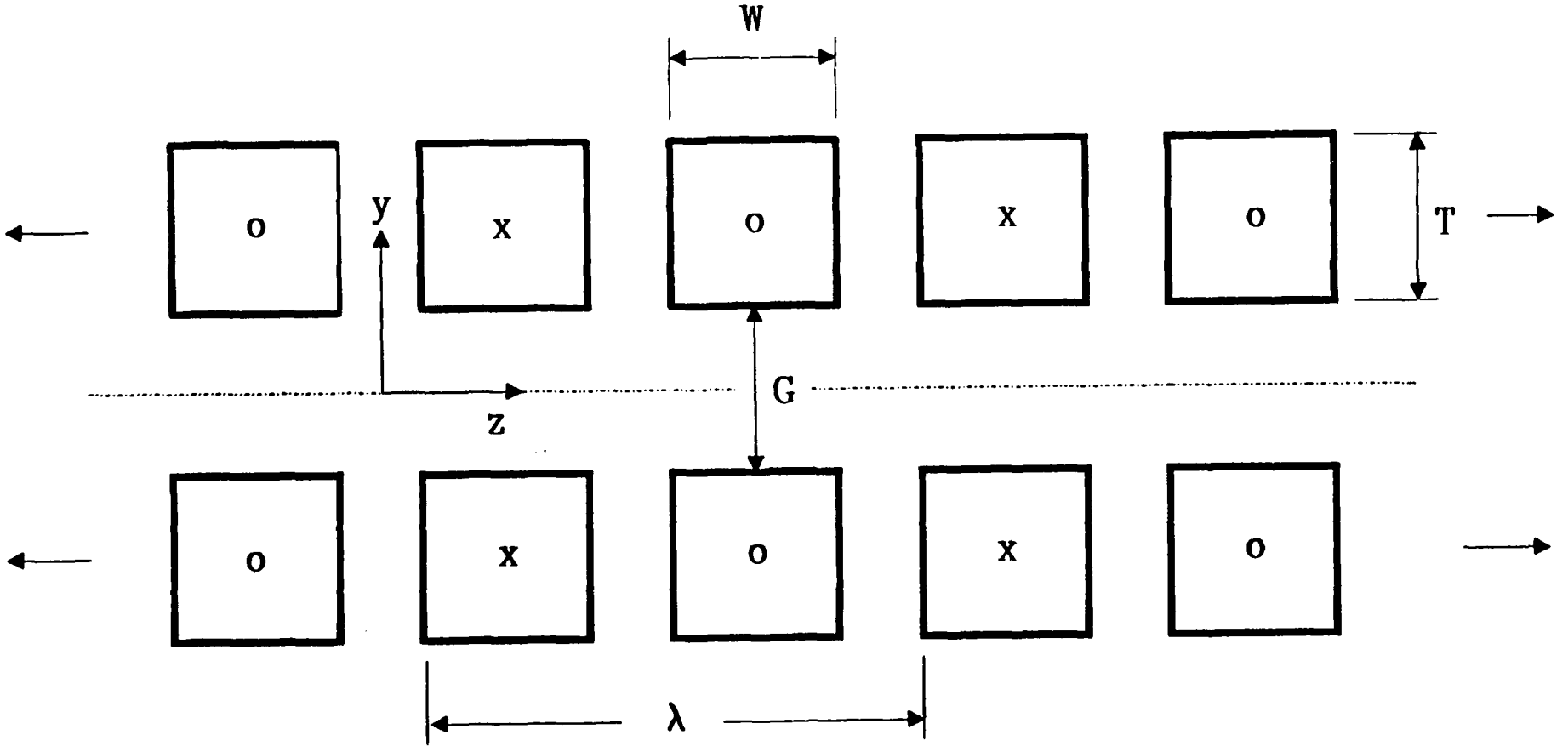

x – Current into paper
o – Current out of paper

Figure 7